Published in final edited form as:
Eur Neuropsychopharmacol. 2014 December ; 24(12): 1896–1906. doi:10.1016/j.euroneuro.2014.10.007.

Dysregulated intracellular signaling in the striatum in a pathophysiologically grounded model of Tourette syndrome

Maximiliano Rapanelli[a,e], **Luciana R. Frick**[a,e], **Vladimir Pogorelov**[a,e,1], **Kristie T. Ota**[a,e], **Eeman Abbasi**[a,e], **Hiroshi Ohtsu**[f], and **Christopher Pittenger**[a,b,c,d,e,*]

[a]Department of Psychiatry, Yale University, New Haven, CT, USA

[b]Department of Psychology, Yale University, New Haven, CT, USA

[c]Child Study Center, Yale University, New Haven, CT, USA

[d]Interdepartmental Neuroscience Program, Yale University, New Haven, CT, USA

[e]Ribicoff Research Facilities, Yale University, New Haven, CT, USA

[f]Tohoku University, Graduate School of Engineering, Sendai, Japan

Abstract

Tic disorders produce substantial morbidity, but their pathophysiology remains poorly understood. Convergent evidence suggests that dysregulation of the cortico-basal ganglia circuitry is central to the pathogenesis of tics. Tourette syndrome (TS), the most severe end of the continuum of tic disorders, is substantially genetic, but causative mutations have been elusive. We recently described a mouse model, the histidine decarboxylase (*Hdc*) knockout mouse, that recapitulates a rare, highly penetrant mutation found in a single family; these mice exhibit TS-like phenomenology. These animals have a global deficit in brain histamine and a consequent dysregulation of DA in the basal ganglia. Histamine modulation of DA effects is increasingly appreciated, but the mechanisms underlying this modulation remain unclear; the consequences of modest DA elevation in the context of profound HA deficiency are difficult to predict, but understanding them in the *Hdc* knockout mouse may provide generalizable insights into the pathophysiology of TS. Here we characterized signaling pathways in striatal cells in this model system, at baseline and after amphetamine challenge. *In vivo* microdialysis confirms elevated DA in *Hdc*-KO mice. We find dephosphorylation of Akt and its target GSK3β and activation of the MAPK signaling cascade and its target rpS6; these are characteristic of the effects of DA on D2- and D1-expressing striatal neurons, respectively. Strikingly, there is no alteration in mTOR signaling, which can be regulated by DA in both cell types. These cellular effects help elucidate striatal signaling abnormalities in a uniquely validated mouse model of TS and move towards the identification of new potential therapeutic targets for tic disorders.

*Corresponding author at: Departments of Psychiatry, Yale University, New Haven, 34 Park Street, W315, New Haven, CT 06519, USA. Tel.: +1 203 974 7675. Christopher.pittenger@yale.edu (C. Pittenger).
[1]Current address: Duke University, Durham, NC, USA

Conflict of interest
The other authors have nothing to disclose.

Keywords

Tourette syndrome; Histamine; Dopamine; Basal ganglia; Striatum

1. Introduction

Tic disorders affect approximately 5% of the population; Tourette syndrome (TS), which lies at the most severe end of the spectrum of tic disorders, has a prevalence of 0.3–1% (Robertson et al., 2009; Williams et al., 2013). Severe cases can cause profound morbidity. The pathophysiology of TS is not well understood, which has retarded the development of new treatments (Williams et al., 2013). Progress has been delayed by the complexity of TS genetics, which has not converged on any clear etiology (Davis et al., 2013; State, 2011), and by the lack of validated, pathophysiologically-grounded animal models in which to test specific hypotheses and generate new molecular insights (Pittenger, 2014).

We recently described a novel animal model of the pathophysiology of TS (Castellan Baldan et al., 2014), based on a rare mutation in the *histidine decarboxylase* (*Hdc*) gene found in a unique family with an exceptionally high incidence of tics (Ercan-Sencicek et al., 2010). Subsequent genetic studies have suggested that dysregulation of HA signaling contributes to TS beyond this index family (Fernandez et al., 2012; Karagiannidis et al., 2012). *Hdc* knockout animals exhibit potentiated tic-like stereotypies when stimulated with D-amphetamine; this is mitigated by systemic injection of the D2 antagonist haloperidol, which is often efficacious in patients with tics, and by direct infusion of HA into the brain. Both knockout animals and patients carrying the *Hdc* mutation also exhibit a deficit in prepulse inhibition, providing further face validity for the model (Castellan Baldan et al., 2014).

Convergent evidence implicates dysfunction of the cortico-basal ganglia circuitry in the pathophysiology of TS (Williams et al., 2013). In particular, dopaminergic excess in this circuitry has been suggested by PET imaging studies (Singer et al., 2002; Wong et al., 2008); the therapeutic efficacy of D2 antagonists (Bloch, 2008) supports the causal importance of this DA excess in the etiology of tics. We therefore focused on the striatal circuitry, and in particular on DA modulation of this circuitry, in the *Hdc* knockout mouse model. *In vivo* micro-dialysis revealed dysregulated DA levels; immunohistochemistry showed elevated expression of the immediate early gene *Fos*, which is regulated by DA in the principle cells of the striatum, the medium spiny neurons (MSNs). Dopamine receptors were elevated in the substantia nigra of both mice and patients carrying a mutated *Hdc* gene, further supporting *in vivo* dysregulation of DA and providing additional translational validation of the model (Castellan Baldan et al., 2014).

Histamine is produced by *Hdc*-expressing cells in the posterior tuberomammilary nucleus of the hypothalamus; these neurons project broadly throughout the brain (Panula and Nuutinen, 2013). The striatum receives a substantial projection from these histaminergic cells (Haas et al., 2008) and contains a disproportionately high amount of HDC protein (Krusong et al., 2011). MSNs express histamine receptors H1R, H2R, and H3R (Haas et al., 2008; Pillot et al., 2002), and histamine modulates the synaptic responses and electrical properties of MSNs in acute brain slices (Ellender et al., 2011). The H3 receptor, in particular, has recently been

revealed as a potentially important regulator of signal transduction in MSNs (Moreno et al., 2011, 2014; Panula and Nuutinen, 2013). The interaction between HA and DA in the modulation of striatal responses is not well understood.

Signaling within MSNs, in response to activity, DA, and other regulators, is complex (Greengard, 2001). Striatal MSNs are separable into those expressing the D1 DA receptor, which project to the substantia nigra pars reticulata (the striatonigral or direct pathway) and those expressing the D2 receptor, which project to the globus pallidus (the striatopallidal or indirect pathway). The dynamic balance between these two pathways is thought to be critical to normal striatal function; it has been hypothesized that imbalance – excessive direct pathway activation and indirect pathway inhibition – is central to the pathogenesis of TS (Albin and Mink, 2006; Baym et al., 2008; Williams et al., 2013). In D1-expresing MSNs, DA leads to elevation of cAMP, activation of PKA and MAPK (ERK) signaling, and activation of DARPP-32 (Bateup et al., 2008; Bertran-Gonzalez et al., 2008; Nishi et al., 2011). In D2-expressing MSNs, DA has the opposite effects on cAMP, PKA, and DARPP-32 (Bateup et al., 2008; Bertran-Gonzalez et al., 2008); it also inhibits Akt via β-arrestin, reducing the phosphorylation of GSK and thereby activating it (Beaulieu et al., 2005). All of these signaling pathways can regulate critical downstream events, including translation and gene expression. For example, the translational regulator ribosomal protein S6 (rpS6) is phosphorylated and activated by the ERK signaling pathway via the kinase ribosomal S6 kinase (RSK1/2) (Frodin and Gammeltoft, 1999), and by the mTOR pathway via its regulation of S6 kinase (S6K) (Magnuson et al., 2012).

Our previous studies establish the *Hdc* knockout mouse as an informative, pathophysiologically-grounded model of at least a rare genetic form of TS (Castellan Baldan et al., 2014). Leveraging of this finding towards generalizable insights into the pathophysiology of TS and, ultimately, towards the development of new treatments requires characterization of how MSN signaling is dysregulated in these mice. The *Hdc* knockout mouse has elevated DA levels, which may increase tonic D1 and D2-regulated signaling, but it also has reduced striatal HA (Castellan Baldan et al., 2014); given the interaction between HA and DA in the regulation of MSN signaling (Bertran-Gonzalez et al., 2008; Moreno et al., 2011, 2014; Panula and Nuutinen, 2013), it is unclear how these two neurochemical abnormalities might interact in altering MSN signal transduction pathways.

We have previously demonstrated that the immediate early gene *Fos*, which is a downstream target of convergent DA-regulated signaling pathways in D1-expressing MSNs, is upregulated in the *Hdc* knockout mouse (Castellan Baldan et al., 2014). Here we examined this and other MSN signaling pathways, to establish which are differentially activated in the TS mouse model. We find evidence for altered signaling in pathways known to be regulated in both striatopallidal and striatonigral neurons, suggesting dysregulation of both direct and indirect pathways in TS.

2. Experimental procedures

2.1. Mice

The generation of *Hdc*-KO mice has been previously described (Ohtsu et al., 2001). These mice have been backcrossed to >10 generations onto the C57Bl/6J genetic background. Knockout mice and wild-type controls were produced by breeding heterozygotes in our vivarium; progeny were genotyped by PCR. Animals were housed in groups of up to five animals per cage with food and water *ad libitum*, with a 12/12 h light/dark cycle, under temperature (23 °C) and humidity-controlled conditions. Two-month-old KO and wild type male mice were used for experimental procedures. All experimental procedures and animal care were approved by and under the supervision of the Yale University Institutional Animal Care and Use Committee.

2.2. *In vivo* microdialysis

DA microdialysis was performed as described in [6]. Mice were surgically implanted unilaterally with guide cannulae targeted to the dorsal striatum (AP + 0.5 mm, ML 2.0 mm, DV − 2.2 mm) under ketamine/xylazine anesthesia, using standard stereotaxic technique, with reference to the atlas of Paxinos (Paxinos and Franklin, 2004). Guide cannulae were affixed to the skull using bilateral skull screws and Cerebond skull fixture adhesive (Plastics One, Roanoke, VA, USA). Dummy cannulae were inserted into the guide cannulae during recovery to ensure patency. Mice recovered from surgery for 3–5 days before continuing with microdialysis.

Following the recovery period, a microdialysis probe (2 mm CMA-7, 6 kDa cutoff; CMA Microdialysis, Stockholm, Sweden) was inserted through the guide cannula to a depth of −3 mm relative to bregma (*i.e.* 2 mm below the tip of the guide cannula), and mice were left in the home cage for 20–24 h. The next day, the probe was connected to a 2.5 ml Hamilton syringe and continuously perfused with artificial cerebrospinal fluid (aCSF; Harvard Apparatus, Holliston, MA, USA) at a rate of 2 μl/min using a programmable infusion pump (CMA Microdialysis, Stockholm, Sweden). Dialysate was collected in 20 μl/10 min fractions on ice and stored at −80 °C for later analysis. Microdialysis was performed in the home cage.

DA was measured using HPLC with electrochemical detection, as described previously (Castellan Baldan et al., 2014). After microdialysis, a small amount of toluidine blue was injected through the cannula; mice were euthanized and their brains removed, sliced, and examined to confirm cannula placement. All cannulae were successfully targeted to the dorsal striatum, as intended.

2.3. Drug administration

Amphetamine (5 mg/kg, Sigma Aldrich) was dissolved in saline solution and administered intraperitoneally. SL-327 (50 mg/kg, Tocris) was resuspended in 20% ethanol and sonicated. Control animals received an equivalent volume of saline or vehicle.

2.4. Western blot analysis

Mice were sacrificed 45 min after amphetamine or saline injection by decapitation, and brains were quickly removed and cooled in ice cold aCSF. The striata of both hemispheres was dissected on an ice-cold surface and then sonicated in RIPA buffer (Cell Signaling Technologies) supplemented with protease inhibitor (cOMPLETE, Roche), phosphatase inhibitors (phosSTOP, Roche) and 2 μM okadaic acid (Millipore). Protein concentration was quantified by bicinchoninic acid protocol (BCA) in accordance with the supplier´s instructions (Pierce). Protein extracts (20 μg) were separated by 7.5% SDS gels (Bio-rad) and then transferred to PVDF membranes with trans-blot turbo transfer system (Bio-rad). Next, membranes were incubated overnight at 4 °C with one the following antibodies (all purchased from Cell Signaling Technologies): diphospho T202/Y204 ERK1/2 (1:2000), phospho T308-AKT (1:1000), phospho S473-AKT (1:1000), phospho S9-GSK3β (1:1000), phospho S235/S236-rpS6 (1:2000) and phospho S2448-mTOR (1:1000). As a control for basal levels of the total amount of protein, membranes were then stripped and re-probed using primary antibodies (all purchased from Cell Signaling Technologies) against AKT (1:1000), ERK1/2 (1:2000), mTOR (1:1000), GSK3β (1:1000) and rpS6 (1:1000). A protein loading control was performed by re-stripping the membranes and then incubating them with an anti-GADPH primary antibody (1:10,000, Millipore). All proteins were detected by using a goat secondary antibody against anti rabbit or mouse primary antibody coupled to peroxidase (1:3000, Vector Laboratories) and developed by ECL (SuperSignal West-Pico, Pierce). Images and data were acquired with Chemidoc XRS system (Bio-rad); analysis was performed using Image J software. Experimental groups were as follows: WT saline (*n*=5), WT amphetamine (*n*=5), *Hdc*-KO saline (*n*=5) and *Hdc*-KO amphetamine (*n*=5).

2.5. Immunohistochemistry

Mice were anesthetized with ketamine/xylazine (100/10 mg/kg) 45 min after amphetamine or saline injection and transcardially perfused with paraformaldehyde (PFA; 4% in PBS). Brains were postfixed overnight in 4% PFA in PBS at 4° and transferred to 30% sucrose for 48 h. Striatal slices were obtained by cutting the brains coronally (30 μM) from A–P levels 1.34 mm to 0.5 mm (Paxinos and Franklin, 2004) using a cryostat (Leica); slices were stored at 4° in a solution containing 30% (vol/vol) ethylene glycol and 30% (vol/vol) glycerol until staining. Striatal slices were rinsed three times in TBS, incubated for 20 min in Bloxall solution (Vector laboratories, USA), washed three times for 10 min in TBS and then blocked for 30 min in 2% NGS in TBS-0.1% triton X-100. Next, samples were incubated overnight at 4 °C with one of the following rabbit primary antibodies against diphospho-T202/Y204 ERK1/2 (1:400; Cell Signaling Technology), phospho-T308-AKT (1:400; Cell Signaling Technology), phospho-S473-AKT (1:200; Cell Signaling Technology), phospho-S9-GSK3β (1:100; Santa Cruz Biotechnology) and phospho-S235/S236-rpS6 (1:800; Cell Signaling Technology). Afterwards, two washes with TBS-0.1% Triton X-100 and one with TBS were performed, section were then incubated with a goat anti rabbit biotinylated secondary antibody for 1 h (1:300, Vector Laboratories). After three washes with TBS-0.1% triton X-100, slices were incubated for 1 h with avidin-coupled horseradish peroxidase complex in TBS (ABC Elite Kit, Vector Laboratories) and then developed with DAB kit (Vector

Laboratories). Four rinses with TBS were performed before counterstaining with nuclear fast red (Vector Laboratories) and mounting.

Positive cells were counted from images of two fields in the dorsal striatum of each hemisphere (without overlap; see Figure S1), acquired using a bright field microscope at 20 × magnification (DM1000, Leica). Two slices per mouse were used per experiment. All positive cells within these regions in both hemispheres were counted. Experimental groups were as follows: WT saline (n=5), WT amphetamine (n=5), *Hdc*-KO saline (n=5), *Hdc*-KO amphetamine (n=5), WT SL-327 (n=5) and Hdc-KO SL-327 (n=5).

2.6. Data analysis

Statistical analysis was performed using GraphPad Prism software. Values are expressed as means ± SEM and compared using Student's *t*-test or two-way or repeated measures two-way ANOVA followed by Sidak's post-hoc test. Differences among experimental conditions were considered statistically significant if $p < 0.05$.

3. Results

3.1. Elevated dopamine in *Hdc*-KO mouse striatum

We have previously shown dopamine dysregulation in the *Hdc*-KO mouse by *in vivo* microdialysis. However, the elevation of DA is subtle, and our previous studies were able to resolve a DA elevation only during the animals' active (dark) phase, when HA levels in WTs are high. On the other hand, elevated striatal *Fos* during the light phase suggested persistent dysregulation [6]. To clarify this, we repeated *in vivo* microdialysis in *Hdc*-KO mice and sibling controls, using re-optimized DA detection by HPLC. We found a modest but significant elevation in striatal DA levels during the day (Figure 1; n=7 WT, 6 *Hdc* KO; p=0.028, 1-tailed *t*-test). This confirms DA dysregulation in the *Hdc* KO mouse.

3.2. Akt signaling is altered in the striatum in the *Hdc*-KO Tourette syndrome model

The kinase Akt is ubiquitously expressed, but it is uniquely regulated in D2-expressing MSNs of the striatopallidal (indirect) pathway through a cAMP-independent, β-arrestin-dependent pathway (Beaulieu et al., 2005). Akt is activated by phosphorylation at T308 by PDK1; D2 activation triggers β-arrestin/PP2A-mediated dephosphorylation of this site (Beaulieu et al., 2009, 2005). We quantified this phosphorylation in *Hdc*-KO mice at baseline and after amphetamine challenge by immunohistochemistry and Western blotting. pAkt-T308-positive cells were decreased in the dorsal striatum in *Hdc*-KO mice (Figure 2A. 2-way ANOVA: main effect of genotype: $F[1,4]=27.31$; p=0.006) and by amphetamine treatment (main effect of amphetamine: $F[1,4]=41.19$; p=0.003). The reduction of pAkt-T308-positive cells in *Hdc*-KO mice was confirmed by Western blotting (Figure 2B. Main effect of genotype, $F[1, 14]=8.700$, p=0.01; main effect for treatment $F[1, 14]=5.067$, p=0.04; treatment × genotype interaction: $F[1, 14]=5.043$, p=0.04). There was no significant reduction in Akt phosphorylation after amphetamine treatment in the *Hdc*-KO mice by Western blot; this suggests a floor effect, wherein the reduction in pAkt-T308 at baseline is such that no further reduction can be measured, at least by this technique.

Akt is also phosphorylated on S473 by the mTORC. However, we found no alterations in pAkt-S473 in *Hdc*-KO mice or after amphetamine by immunohistochemistry (Figure 2C) or Western blotting (Figure 2D), confirming the specificity of the observed alterations in pAKT-T308.

3.3. Reduced pAkt-T308 is accompanied by altered activation of GSK3β but not mTOR

Akt regulates numerous downstream effectors (Beaulieu et al., 2009; Hemmings and Restuccia, 2012). Prominent among these are GSK3β and mTOR. We examined these substrates to better characterize the consequences of Akt dysregulation in the *Hdc*- KO model.

Akt deactivates GSK3β by phosphorylation at S9; reduced Akt activity (Figure 2) is thus predicted to lead to decreased pGSK3β-S9, which would correspond to increased GSK3β activity. Consistent with this prediction, immunohistochemical analysis revealed decreased pGSK3β-S9-positive neurons in the dorsal striatum in *Hdc*-KO mice (Figure 3A; 2-way ANOVA: main effect of genotype: $F[1,4]=34.98$; $p=0.001$) and after amphetamine treatment (main effect of amphetamine: $F[1,6]=134.9$; $p<0.0001$; genotype × amphetamine interaction: $F[1,4]=21.46$; $p=0.004$). Amphetamine treatment eliminated the genotype effect on pGSK3β-S9. These effects were confirmed by Western blotting for pGSK3β-S9. We found reduced levels of pGSK3β-S9 in *Hdc*-KO mice and after amphetamine treatment (Figure 3B; main effect of genotype: $F[1,14]=12.1$; $p=0.003$; main effect of amphetamine: $F[1,14]=7.154$; $p=0.02$; genotype × amphetamine interaction: $F[1,14]=11.92$; $p=0.003$).

Akt also regulates signaling through the ubiquitous mTOR complex via inhibitory phosphorylation of TSC2 and PRAS40 (Manning and Cantley, 2007). One read-out of mTOR activity is phosphorylation of S2448, which is a substrate for the mTOR-regulated S6 kinase (Chiang and Abraham, 2005; Holz and Blenis, 2005). However, we found no alteration in pmTOR-S2448 in *Hdc*-KO mice, with or without amphetamine treatment (Figure 3C; 2-way ANOVA; main effect for treatment $F[1,14]=0.28$, $p=0.6$; main effect for genotype $F[1,14]=0.15$, $p=0.7$; genotype × treatment interaction $F[1,14]=0.5093$, $p=0.5$). We also examined phosphorylation of riboprotein S6 (rpS6) at site S240/244 which is a target of S6K and is positively regulated by pmTOR-S2448; again, there was no alteration in *Hdc*-KO mice, with or without amphetamine treatment (Figure 3D; 2 way ANOVA; main effect of amphetamine: $F[1,14]=0.7$, $p=0.4$; main effect of genotype: $F[1,16]=0.79$, $p=0.4$; genotype × amphetamine interaction: $F[1,16]=2.344$, $p=0.15$).

3.4. MAPK signaling is altered in the *Hdc*-KO Tourette syndrome model

Signaling through the MAPK pathway is activated in D1-expressing striatonigral MSNs by neural activity and by cAMP- and DARPP-32-dependent modulation of phosphatases (Bateup et al., 2008; Beaulieu et al., 2009; Bertran-Gonzalez et al., 2008; Nishi et al., 2011). We examined the activation of ERK1/2 MAP kinase by phosphorylation at T202 and Y204. pERK1/2-positive cells in the dorsal striatum were increased in *Hdc*-KO mice and after amphetamine (Figure 4A; 2-way ANOVA: main effect of genotype: $F[1,4]=8.512$, $p=0.04$; main effect of amphetamine: $F[1,4]=96.28$; $p<0.001$; genotype × amphetamine interaction:

$F[1,4]=26.59$; $p=0.007$). Main effects of genotype ($F[1,14]=10.47$; $p=0.006$) and amphetamine ($F[1,14]=130.7$; $p<0.0001$) were confirmed by Western blotting (Figure 4B).

MAPK regulates translation through its regulation of rpS6 via RSK-mediated phosphorylation of S235/236 (Frodin and Gammeltoft, 1999). We found an increase in phosphorylated rpS6-S235/236-positive cells in the dorsal striatum in *Hdc*-KO mice (Figure 5A; 2-way ANOVA: main effect of genotype: $F[1,4]=19.93$; $p=0.01$) and after amphetamine (main effect of amphetamine: $F[1,4]=39.20$; $p=0.004$). Of note, S235/236 is also an mTOR target. S240/244 (whose phosphorylation is not altered in these animals; Figure 3C and D) is an mTOR but not a MAPK target. The specificity of the increased S235/236 phosphorylation we observe suggests that it is due to MAPK, not mTOR. To further corroborate this, we repeated this experiment with the potent ERK kinase (MEK) inhibitor SL-327. The inhibitor strongly reduced rpS6-S235/236 in both genotypes (Figure 5B; main effect of genotype: $F[1,4]=79.07$, $p=0.001$; main effect of SL-327: $F[1,4]=222.9$, $p=0.0001$; genotype × SL-327 interaction: $F[1,4]=8.557$, $p=0.04$). Elevated rpS6-S235/236 in *Hdc*-KO mice was confirmed by Western blotting: there was a significant increase in phospho-rpS6-S235/236 in *Hdc*-KO mice and after amphetamine (Figure 5C; 2-way ANOVA: main effect of genotype: $F[1,14]=16.78$; $p=0.0008$; main effect of amphetamine: $F[1,41]=54.42$; $p<0.0001$; genotype × amphetamine interaction: $F[1,14]=12.64$; $p=0.003$).

4. Discussion

The molecular mechanisms underlying TS are poorly understood (Williams et al., 2013); this limits efforts to develop new, pathophysiologically-informed treatments. In this context, the identification of a mutation in *Hdc* that appears to be a rare, high-penetrance genetic cause (Ercan-Sencicek et al., 2010) and the validation of the *Hdc* knockout mouse as a pathophysiologically-informed animal model (Castellan Baldan et al., 2014) are landmark events. Identification of molecular and cellular alterations in such an animal model holds great promise for advancing our understanding of the disorder more generally and for the identification of novel treatment targets. We examined dopamine and DA-regulated signal transduction pathways in striatal MSNs in the *Hdc* knockout model. We find alterations of both AKT and MAPK signaling.

Hdc-KO mice have elevated DA (Figure 1; (Castellan Baldan et al., 2014)) and increased DA turnover (Dere et al., 2003) in the striatum. This recapitulates DA dysregulation revealed by PET imaging in patients with TS (Singer et al., 2002; Wong et al., 2008). Abnormalities in signaling in these animals may therefore simply reflect increased basal stimulation of D1 and/or D2 DA receptors. Alternatively, abnormalities in MSN signaling may result from changes in other signaling pathways in the absence of normal HA stimulation, or from a conjunction of events.

AKT is ubiquitously expressed but is uniquely regulated in D2-positive MSNs via a β-arrestin-dependent mechanism. It is activated by PI3K by phosphorylation at S473 and T308 (Beaulieu and Gainetdinov, 2011). When phosphorylated on T308, AKT phosphorylates GSK3β, thereby inactivating it (Jacinto et al., 2006). Activation of D2 and D3 receptors in the striatum leads to dephosphorylation of AKT T308; reduced AKT activity leads to

reduced phosphorylation (and therefore increased activity) of GSK3β (Beaulieu et al., 2004, 2005). We see a similar baseline change in the *Hdc*-KO TS model, with decreased pT308-AKT and pS9-GSK3β. In contrast, AKT phosphorylation at S473 is not altered in *Hdc*-KO mice, or after amphetamine. There was some specificity to the downstream effects of activated AKT on GSK3β: the activity of mTOR, which can also be regulated by AKT, was not altered in these mice.

These alterations may result from increased D2 activation by elevated DA in these mice; D1 receptors are not believed to regulate AKT (Beaulieu et al., 2007). Hyperdopaminergic dopamine transporter KO mice (DAT-KO) also have reduced pT308-AKT and pS9-GSK3β in the striatum (Beaulieu et al., 2004), supporting the sufficiency of elevated DA to produce these effects. In DAT-KO mice, cell-specific deletion of GSK3β in D2-expressing MSNs eliminates the elevation in locomotion (Urs et al., 2012), supporting the causal importance of this abnormality; GSK3β deletion in D1-expressing MSNs does not have this effect. GSK3β activity has been implicated in other psychiatric disorders, though not previously in Tourette syndrome (Emamian et al., 2004; Prickaerts et al., 2006). GSK3β is inhibited by lithium and other mood stabilizers and is a major target for ongoing efforts at drug development. It is also phosphorylated, and therefore presumably inhibited, by treatment with haloperidol, which is an efficacious pharmacotherapy for TS (Sutton and Rushlow, 2011). The observation of hypophosphorylated (and therefore presumptively hyperactive) GSK3β in this animal model of TS suggests that it may be a potential treatment target.

We also observe increased levels of pT202/Y204-ERK1/2 in the striatum of *Hdc*-KO mice, and after amphetamine challenge. ERK1/2 is activated by phosphorylation in D1-expressing cells after amphetamine in wild-type mice; this activation leads to the increased expression of the immediate-early genes *c-fos* and *zif268* (Gerfen et al., 2008; Girault et al., 2007). This ERK1/2 activation may therefore underlie the upregulated *c-fos* that we have previously observed in these animals, both at baseline and after amphetamine challenge (Castellan Baldan et al., 2014). In this case, elevation of DA in these animals (Figure 1) may not be a sufficient explanation for the activation of ERK1/2. In wild-type mice, D1 activation is not sufficient for ERK 1/2 activation (Gerfen et al., 2002); activation after amphetamine also depends on the activation of glutamate receptors (Valjent et al., 2005). Activation of postsynaptic H3 receptors inhibits activation of MAPK by D1 receptors, at least in reduced systems (Moreno et al., 2011, 2014). Loss of this inhibitory mechanism in these animals may lead to MAPK activation that would not be produced by DA elevation in the context of normal HA levels. Alternatively, chronic disinhibition of glutamate release due to loss of presynaptic H3 tone (Ellender et al., 2011) may provide the increased glutamate required for MAPK activation (Valjent et al., 2005).

ERK1/2 activation can lead to multiple downstream effects on other kinases and transcription factors in D1-expressing MSNs. Downstream targets include mTOR, RSK1/2 and MSK1; these in turn regulate gene expression and protein synthesis through mechanisms including the phosphorylation of rpS6 and histone H3 (Brami-Cherrier et al., 2005; Girault et al., 2007). We found elevated pS235/S236-rpS6 in the *Hdc*-KO mice; this phosphorylation was further augmented after amphetamine (Figure 5). The regulation of rpS6 appears to be specific to the MAPK/RSK pathway: the S240/S244 site, an mTOR

target (Roux et al., 2007), was not altered in *Hdc*-KO mice (Figure 3D), and the increased phosphorylation of the S240/S244 site was abolished by the MAPK-kinase inhibitor SL327 (Figure 5A).

These experiments cannot definitively assign the observed signaling abnormalities to D1 or D2 MSNs; these two cell types are comingled in our immunohistochemical staining and Western blots. However, in the context of previous work, it seems likely that the two signaling effects we observe map onto these two cell populations. As noted above, AKT is regulated by D2 receptors but is not regulated by DA in D1-expressing MSNs; ERK, on the other hand, is activated by DA in D1-expressing but not in D2-expressing MSNs. We hypothesize, correspondingly, that the baseline abnormalities in AKT and GSK3β that we observe are specific to D2-expressing striatopallidal pathway MSNs, and the ERK and rpS6 phosphorylation is specific to D1-expressing cells of the striatonigral pathway. Replication of these results in animals with cell type-specific labels will be required to test these hypotheses. Such a pattern would be consistent with a model in which TS is caused by increased activation of motor patterns via the striatonigral pathway and decreased inhibition of off-target motor patterns via hypoactivity of the striatopallidal pathway (Williams et al., 2013).

The ultimate value of pathophysiologically-grounded animal models of neuropsychiatric disease lies in their ability to reveal potential mechanisms of pathology that are not accessible in patients. We have previously validated the *Hdc*-KO mouse as a valuable model of the pathophysiology of TS. Here we have used this model to identify specific abnormalities in basal ganglia signaling in this model. Our analysis reveals one potential therapeutic target, GSK3β. Translational extension of these findings holds promise for the development of novel therapeutic strategies for the treatment of TS and other tic disorders.

Acknowledgements

The authors gratefully acknowledge Stacey Wilber for mouse genotyping and technical assistance, and Angus Nairn and Ron Duman for valuable discussion and critical input. This work was supported by the Allison Family Foundation (CP), F32MH098513 (KO), and by the State of Connecticut through its support of the Ribicoff Research Facilities at the Connecticut Mental Health Center.

Dr. Pittenger has received consultancy fees and research funding from F. Hoffman La Roche, Ltd., and educational grants from F. Hoffman la Roche, Ltd. and Medtronic, Inc.

Role of the funding source

This work was funded by The Allison Family Foundation, NIH grant F32MH098513, and the State of Connecticut. The funders played no role in the design, execution, or interpretation of these experiments or in preparing the manuscript.

References

Albin RL, Mink JW. Recent advances in Tourette syndrome research. Trends Neurosci. 2006; 29:175–182. [PubMed: 16430974]

Bateup HS, Svenningsson P, Kuroiwa M, Gong S, Nishi A, Heintz N, Greengard P. Cell type-specific regulation of DARPP-32 phosphorylation by psychostimulant and antipsychotic drugs. Nat. Neurosci. 2008; 11:932–939. [PubMed: 18622401]

Baym CL, Corbett BA, Wright SB, Bunge SA. Neural correlates of tic severity and cognitive control in children with Tourette syndrome. Brain: a journal of neurology. 2008; 131:165–179. [PubMed: 18056159]

Beaulieu JM, Gainetdinov RR. The physiology, signaling, and pharmacology of dopamine receptors. Pharmacol. Rev. 2011; 63:182–217. [PubMed: 21303898]

Beaulieu JM, Gainetdinov RR, Caron MG. Akt/GSK3 signaling in the action of psychotropic drugs. Annu. Rev. Pharmacol. Toxicol. 2009; 49:327–347. [PubMed: 18928402]

Beaulieu JM, Sotnikova TD, Marion S, Lefkowitz RJ, Gainetdinov RR, Caron MG. An Akt/beta-arrestin 2/PP2A signaling complex mediates dopaminergic neurotransmission and behavior. Cell. 2005; 122:261–273. [PubMed: 16051150]

Beaulieu JM, Sotnikova TD, Yao WD, Kockeritz L, Woodgett JR, Gainetdinov RR, Caron MG. Lithium antagonizes dopamine-dependent behaviors mediated by an AKT/glycogen synthase kinase 3 signaling cascade. Proc. Natl. Acad. Sci. U.S.A. 2004; 101:5099–5104. [PubMed: 15044694]

Beaulieu JM, Tirotta E, Sotnikova TD, Masri B, Salahpour A, Gainetdinov RR, Borrelli E, Caron MG. Regulation of Akt signaling by D2 and D3 dopamine receptors *in vivo*. J. Neurosci.: the official journal of the Society for Neuroscience. 2007; 27:881–885.

Bertran-Gonzalez J, Bosch C, Maroteaux M, Matamales M, Herve D, Valjent E, Girault JA. Opposing patterns of signaling activation in dopamine D1 and D2 receptor-expressing striatal neurons in response to cocaine and haloperidol. J. Neurosci.: the official journal of the Society for Neuroscience. 2008; 28:5671–5685.

Bloch MH. Emerging treatments for Tourette's disorder. Curr. Psychiatry Rep. 2008; 10:323–330. [PubMed: 18627671]

Brami-Cherrier K, Valjent E, Herve D, Darragh J, Corvol JC, Pages C, Arthur SJ, Girault JA, Caboche J. Parsing molecular and behavioral effects of cocaine in mitogen- and stress-activated protein kinase-1-deficient mice. J. Neurosci.: the official journal of the Society for Neuroscience. 2005; 25:11444–11454.

Castellan Baldan L, Williams KA, Gallezot JD, Pogorelov V, Rapanelli M, Crowley M, Anderson GM, Loring E, Gorczyca R, Billingslea E, et al. Histidine decarboxylase deficiency causes Tourette syndrome: parallel findings in humans and mice. Neuron. 2014; 81:77–90. [PubMed: 24411733]

Chiang GG, Abraham RT. Phosphorylation of mammalian target of rapamycin (mTOR) at Ser-2448 is mediated by p70S6 kinase. J. Biol. Chem. 2005; 280:25485–25490. [PubMed: 15899889]

Davis LK, Yu D, Keenan CL, Gamazon ER, Konkashbaev AI, Derks EM, Neale BM, Yang J, Lee SH, Evans P, et al. Partitioning the heritability of Tourette syndrome and obsessive compulsive disorder reveals differences in genetic architecture. PLos Genet. 2013; 9:e1003864. [PubMed: 24204291]

Dere E, De Souza-Silva MA, Topic B, Spieler RE, Haas HL, Huston JP. Histidine-decarboxylase knockout mice show deficient nonreinforced episodic object memory, improved negatively reinforced water-maze performance, and increased neo- and ventro-striatal dopamine turnover. Learn. Memory. 2003; 10:510–519.

Ellender TJ, Huerta-Ocampo I, Deisseroth K, Capogna M, Bolam JP. Differential modulation of excitatory and inhibitory striatal synaptic transmission by histamine. J. Neurosci.: the official journal of the Society for Neuroscience. 2011; 31:15340–15351.

Emamian ES, Hall D, Birnbaum MJ, Karayiorgou M, Gogos JA. Convergent evidence for impaired AKT1-GSK3beta signaling in schizophrenia. Nat. Genet. 2004; 36:131–137. [PubMed: 14745448]

Ercan-Sencicek AG, Stillman AA, Ghosh AK, Bilguvar K, O'Roak BJ, Mason CE, Abbott T, Gupta A, King RA, Pauls DL, et al. l-Histidine decarboxylase and Tourette's syndrome. N. Engl. J. Med. 2010; 362:1901–1908. [PubMed: 20445167]

Fernandez TV, Sanders SJ, Yurkiewicz IR, Ercan-Sencicek AG, Kim YS, Fishman DO, Raubeson MJ, Song Y, Yasuno K, Ho WS, et al. Rare copy number variants in Tourette syndrome disrupt genes in histaminergic pathways and overlap with autism. Biol. Psychiatry. 2012; 71:392–402. [PubMed: 22169095]

Frodin M, Gammeltoft S. Role and regulation of 90 kDa ribosomal S6 kinase (RSK) in signal transduction. Mol. Cell. Endocrinol. 1999; 151:65–77. [PubMed: 10411321]

Gerfen CR, Miyachi S, Paletzki R, Brown P. D1 dopamine receptor supersensitivity in the dopamine-depleted striatum results from a switch in the regulation of ERK1/2/MAP kinase. J. Neurosci.the official journal of the Society for Neuroscience. 2002; 22:5042–5054.

Gerfen CR, Paletzki R, Worley P. Differences between dorsal and ventral striatum in Drd1a dopamine receptor coupling of dopamine- and cAMP-regulated phosphoprotein-32 to activation of extracellular signal-regulated kinase. J. Neurosci.: the official journal of the Society for Neuroscience. 2008; 28:7113–7120.

Girault JA, Valjent E, Caboche J, Herve D. ERK2: a logical AND gate critical for drug-induced plasticity? Curr. Opin. Pharmacol. 2007; 7:77–85. [PubMed: 17085074]

Greengard P. The neurobiology of dopamine signaling. Biosci. Rep. 2001; 21:247–269. [PubMed: 11892993]

Haas HL, Sergeeva OA, Selbach O. Histamine in the nervous system. Physiol. Rev. 2008; 88:1183–1241. [PubMed: 18626069]

Hemmings BA, Restuccia DF. PI3K-PKB/Akt pathway. Cold Spring Harbor Perspect. Biol. 2012; 4:a011189.

Holz MK, Blenis J. Identification of S6 kinase 1 as a novel mammalian target of rapamycin (mTOR)-phosphorylating kinase. J. Biol. Chem. 2005; 280:26089–26093. [PubMed: 15905173]

Jacinto E, Facchinetti V, Liu D, Soto N, Wei S, Jung SY, Huang Q, Qin J, Su B. SIN1/MIP1 maintains rictor-mTOR complex integrity and regulates Akt phosphorylation and substrate specificity. Cell. 2006; 127:125–137. [PubMed: 16962653]

Karagiannidis I, Rizzo R, Tarnok Z, Wolanczyk T, Hebebrand J, Nothen MM, Lehmkuhl G, Farkas L, Nagy P, Barta C, et al. Replication of association between a SLITRK1 haplotype and Tourette Syndrome in a large sample of families. Mol. Psychiatry. 2012; 17:665–668. [PubMed: 22083730]

Krusong K, Ercan-Sencicek AG, Xu M, Ohtsu H, Anderson GM, State MW, Pittenger C. High levels of histidine decarboxylase in the striatum of mice and rats. Neurosci. Lett. 2011; 495:110–114. [PubMed: 21440039]

Magnuson B, Ekim B, Fingar DC. Regulation and function of ribosomal protein S6 kinase (S6K) within mTOR signalling networks. Biochem. J. 2012; 441:1–21. [PubMed: 22168436]

Manning BD, Cantley LC. AKT/PKB signaling: navigating downstream. Cell. 2007; 129:1261–1274. [PubMed: 17604717]

Moreno E, Hoffmann H, Gonzalez-Sepulveda M, Navarro G, Casado V, Cortes A, Mallol J, Vignes M, McCormick PJ, Canela EI, et al. Dopamine D1-histamine H3 receptor heteromers provide a selective link to MAPK signaling in GABAergic neurons of the direct striatal pathway. J. Biol. Chem. 2011; 286:5846–5854. [PubMed: 21173143]

Moreno E, Moreno-Delgado D, Navarro G, Hoffmann HM, Fuentes S, Rosell-Vilar S, Gasperini P, Rodriguez-Ruiz M, Medrano M, Mallol J, et al. Cocaine disrupts histamine H3 receptor modulation of dopamine D1 receptor signaling: sigma1-D1-H3 receptor complexes as key targets for reducing cocaine's effects. J. Neurosci.: the official journal of the Society for Neuroscience. 2014; 34:3545–3558.

Nishi A, Kuroiwa M, Shuto T. Mechanisms for the modulation of dopamine d(1) receptor signaling in striatal neurons. Front. Neuroanat. 2011; 5:43. [PubMed: 21811441]

Ohtsu H, Tanaka S, Terui T, Hori Y, Makabe-Kobayashi Y, Pejler G, Tchougounova E, Hellman L, Gertsenstein M, Hirasawa N, et al. Mice lacking histidine decarboxylase exhibit abnormal mast cells. FEBS Lett. 2001; 502:53–56. [PubMed: 11478947]

Panula P, Nuutinen S. The histaminergic network in the brain: basic organization and role in disease. Nat. Rev. Neurosci. 2013; 14:472–487. [PubMed: 23783198]

Paxinos, G.; Franklin, KBJ. The mouse brain in stereotaxic coordinates, Compact. second ed.. Boston: Elsevier Academic Press, Amsterdam; 2004.

Pillot C, Heron A, Cochois V, Tardivel-Lacombe J, Ligneau X, Schwartz JC, Arrang JM. A detailed mapping of the histamine H(3) receptor and its gene transcripts in rat brain. Neuroscience. 2002; 114:173–193. [PubMed: 12207964]

Pittenger, C. Animal models of Tourette syndrome and obsessive-compulsive disorder. In: LeDoux, ME., editor. Animal Models of Movement Disorders. New York: Elsevier; 2014.

Prickaerts J, Moechars D, Cryns K, Lenaerts I, van Craenendonck H, Goris I, Daneels G, Bouwknecht JA, Steckler T. Transgenic mice overexpressing glycogen synthase kinase 3beta: a putative model of hyperactivity and mania. J. Neurosci.: the official journal of the Society for Neuroscience. 2006; 26:9022–9029.

Robertson MM, Eapen V, Cavanna AE. The international prevalence, epidemiology, and clinical phenomenology of Tourette syndrome: a cross-cultural perspective. J. Psychosom. Res. 2009; 67:475–483. [PubMed: 19913651]

Roux PP, Shahbazian D, Vu H, Holz MK, Cohen MS, Taunton J, Sonenberg N, Blenis J. RAS/ERK signaling promotes site-specific ribosomal protein S6 phosphorylation via RSK and stimulates cap-dependent translation. J. Biol. Chem. 2007; 282:14056–14064. [PubMed: 17360704]

Singer HS, Szymanski S, Giuliano J, Yokoi F, Dogan AS, Brasic JR, Zhou Y, Grace AA, Wong DF. Elevated intrasynaptic dopamine release in Tourette's syndrome measured by PET. Am. J. Psychiatry. 2002; 159:1329–1336. [PubMed: 12153825]

State MW. The genetics of Tourette disorder. Curr. Opin. Genet. Dev. 2011; 21:302–309. [PubMed: 21277193]

Sutton LP, Rushlow WJ. The effects of neuropsychiatric drugs on glycogen synthase kinase-3 signaling. Neuroscience. 2011; 199:116–124. [PubMed: 22001305]

Urs NM, Snyder JC, Jacobsen JP, Peterson SM, Caron MG. Deletion of GSK3beta in D2R-expressing neurons reveals distinct roles for beta-arrestin signaling in antipsychotic and lithium action. Proc. Natl. Acad. Sci. U.S.A. 2012; 109:20732–20737. [PubMed: 23188793]

Valjent E, Pascoli V, Svenningsson P, Paul S, Enslen H, Corvol JC, Stipanovich A, Caboche J, Lombroso PJ, Nairn AC, et al. Regulation of a protein phosphatase cascade allows convergent dopamine and glutamate signals to activate ERK in the striatum. Proc. Natl. Acad. Sci. U.S.A. 2005; 102:491–496. [PubMed: 15608059]

Williams, K.; Bloch, MH.; State, MW.; Pittenger, C. Tourette syndrome and tic disorders. In: Charney, DS.; Buxbaum, JD.; Sklar, P.; Nestler, EJ., editors. In Neurobiology of Mental Illness. fourth ed.. New York: Oxford; 2013.

Wong DF, Brasic JR, Singer HS, Schretlen DJ, Kuwabara H, Zhou Y, Nandi A, Maris MA, Alexander M, Ye W, et al. Mechanisms of dopaminergic and serotonergic neurotransmission in Tourette syndrome: clues from an *in vivo* neurochemistry study with PET. Neuropsychopharmacology. 2008; 33:1239–1251. [PubMed: 17987065]

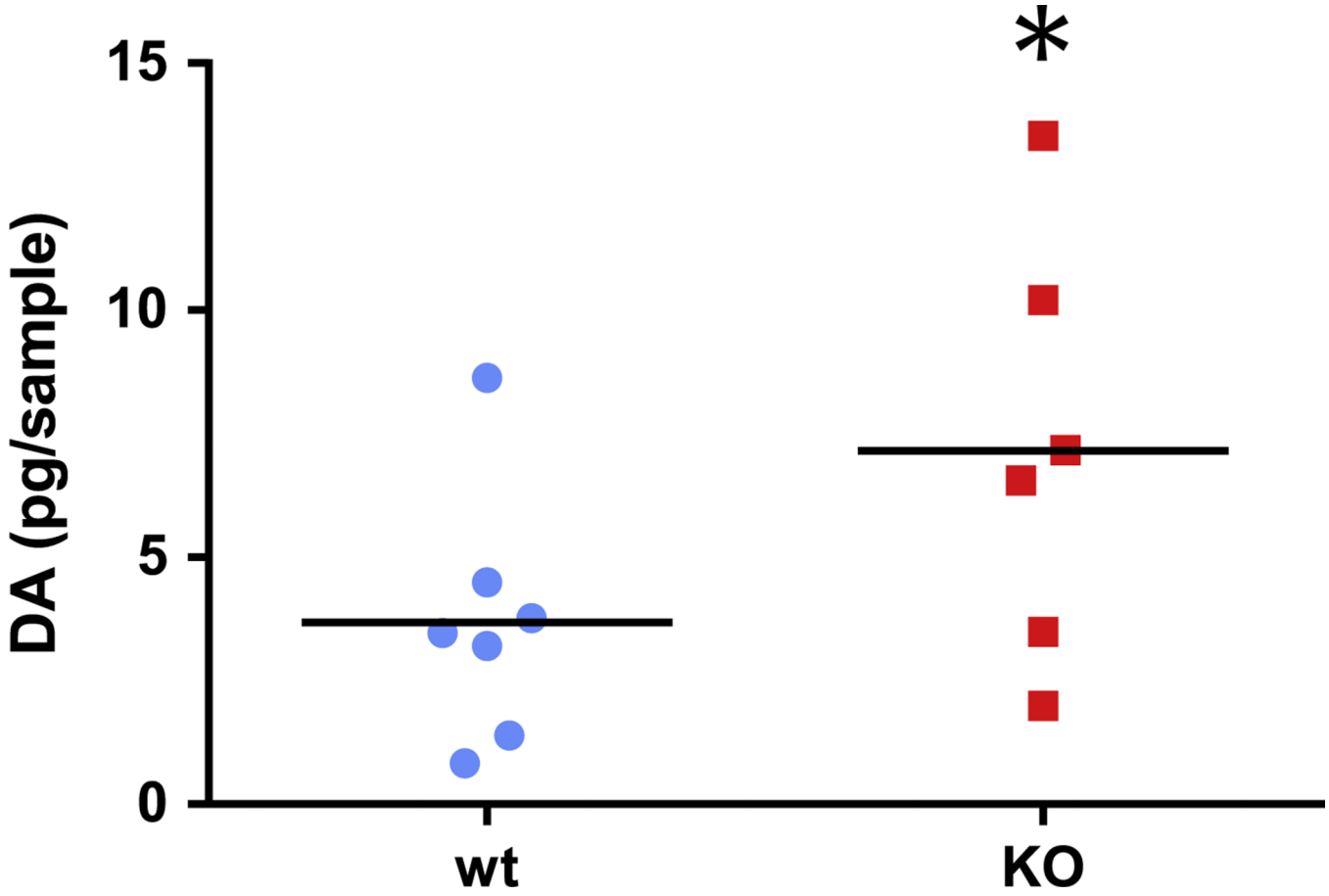

Figure 1.

Basal DA is elevated in the dorsal striatum in *Hdc* KO mice. DA in striatal microdialysate from the dorsal striatum [6] was assayed during the day using HPLC. *Hdc* KO mice had elevated unnormalized DA, relative to littermate controls. Individual datapoints and means are shown (n=7 WT, 6 *Hdc* KO; p<0.03, 1-tailed t-test).

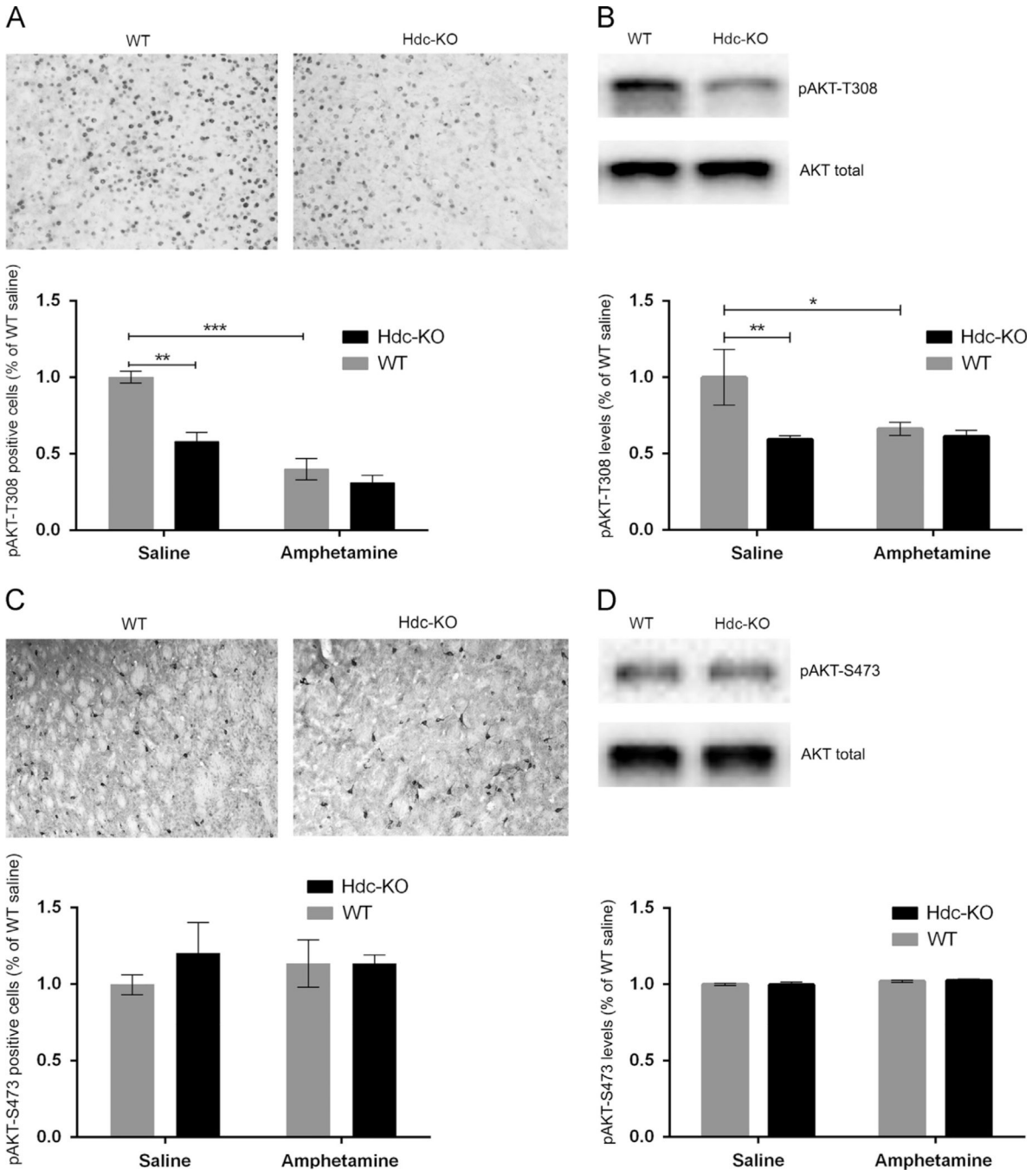

Figure 2.

AKT signaling in *Hdc* KO mice. (A) Phospho-T308 AKT was immunostained in fixed cryostat slices from WT and KO mice, treated with either saline or amphetamine; cells were counted blind to genotype and condition. pT308-AKT-positive cells were decreased in *Hdc*-KO mice and by amphetamine pretreatment (main effect of genotype: $F[1,4]=27.31$; $p=0.006$; main effect of amphetamine: $F[1,4]=41.19$; $p=0.003$). (B) Reduced pT308-AKT was also seen in *Hdc*-KO mice by Western blot (main effect of genotype, $F[1, 14]=8.700$, $p=0.01$; main effect for treatment $F[1, 14]=5.067$, $p=0.04$; treatment × genotype interaction:

F[1, 14]=5.043, *p*=0.04). (C) and (D) Phospho-S473 AKT was not altered by genotype or amphetamine pretreatment, as measured by immunohistochemistry or Western blotting (C and D, respectively; main effects and interactions not significant).

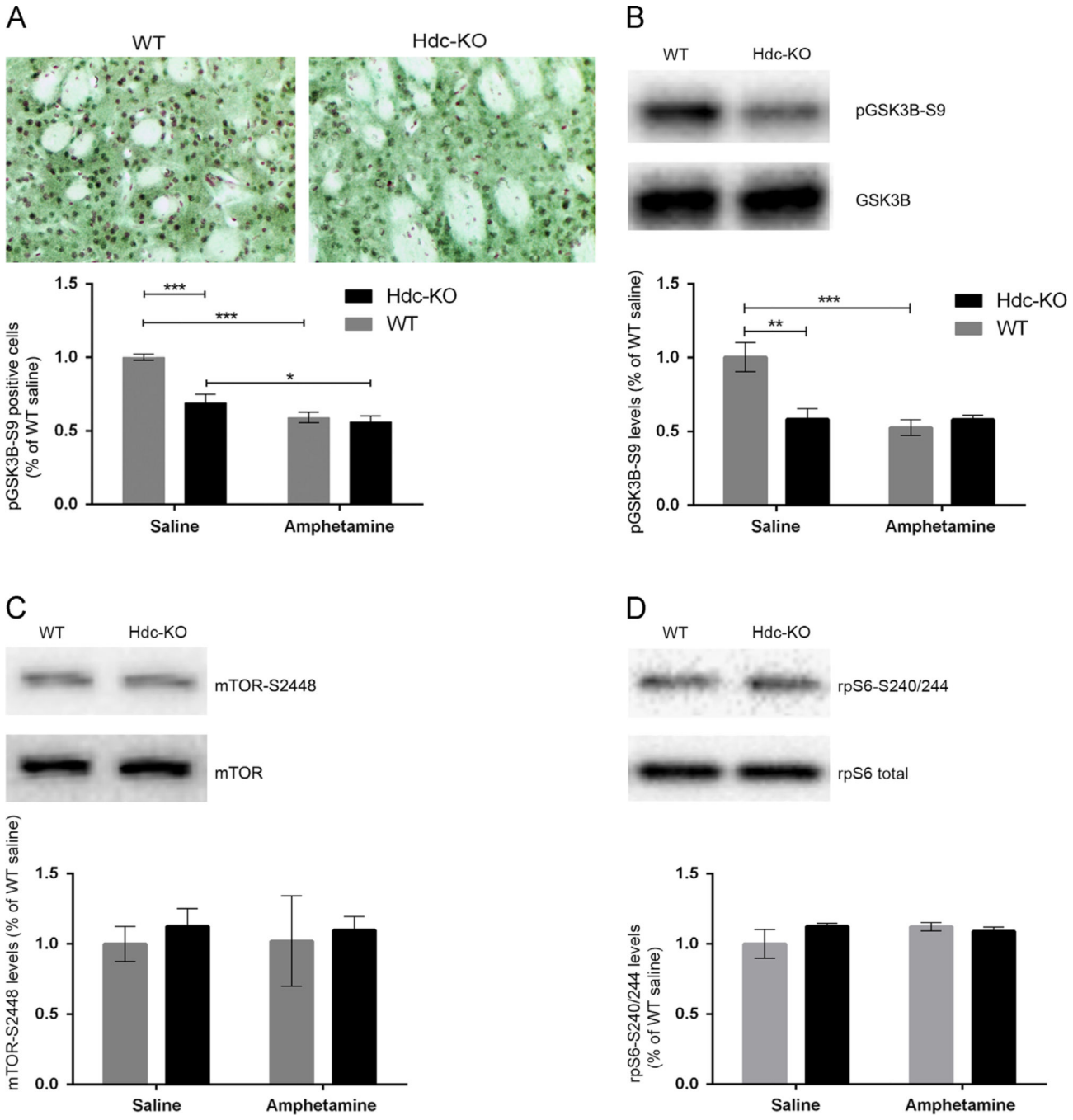

Figure 3.

AKT targets in *Hdc* KO mice. (A) Phospho-S9-GSK3β, measured by immunohistochemistry and cell counting in the dorsal striatum by an observer blind to genotype and condition, was reduced in *Hdc*-KO mice and after amphetamine (2-way ANOVA: main effect of genotype: $F[1,4]=34.98$; $p=0.001$; main effect of amphetamine: $F[1,6]=134.9$; $p<0.0001$; genotype × amphetamine interaction: $F[1,4]=21.46$; $p=0.004$). (B) This reduced pS9-GSK3β was confirmed by Western blotting (main effect of genotype: $F[1,14]=12.1$; $p=0.003$; main effect of amphetamine: $F[1,14]=7.154$; $p=0.02$; genotype × amphetamine interaction:

F[1,14]=11.92; *p*=0.003). (C) Phospho-S2448-mTOR, a marker of mTOR activity, was not altered by *Hdc* genotype or by amphetamine pretreatment (all main effects and interactions not significant). (D) phospho-S240/244-rpS6, which is regulated by mTOR, was not altered by *Hdc* genotype or by amphetamine pretreatment (all main effects and interactions not significant).

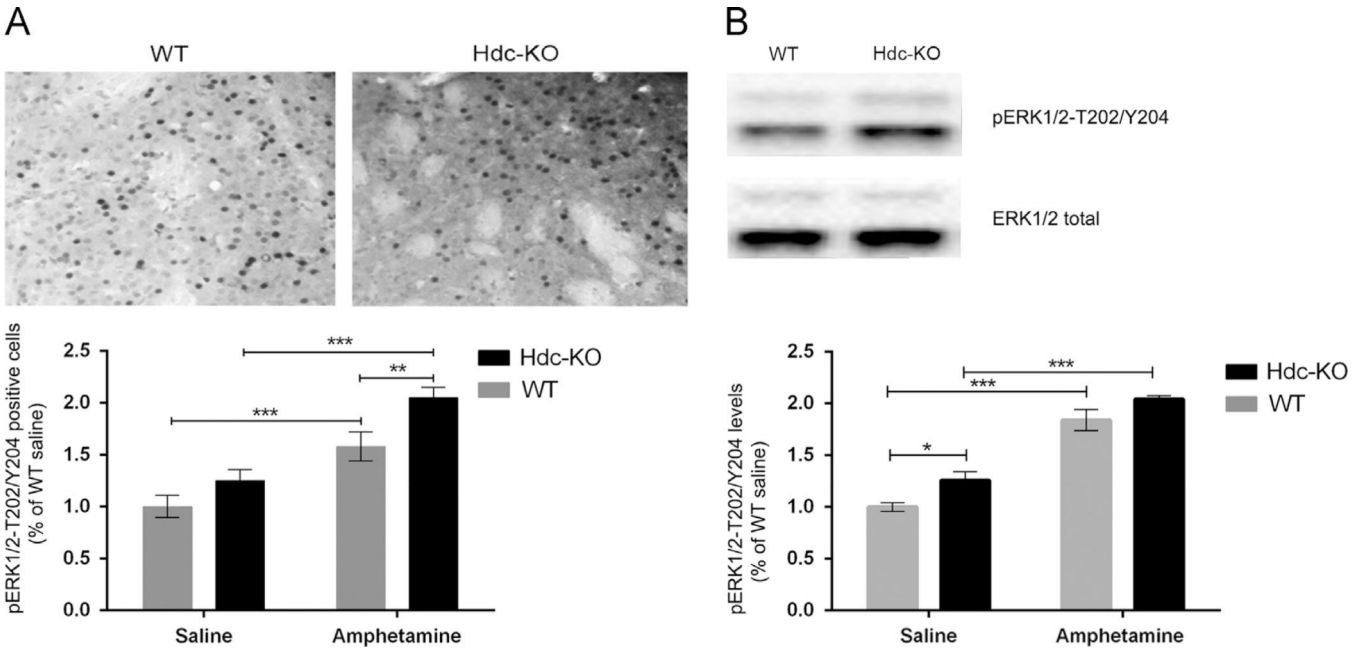

Figure 4.

MAPK signaling in *Hdc*-KO mice. (A) Phospho-T202/Y204-ERK1/2, measured in the dorsal striatum by immunostaining and cell counting by an observer blind to genotype and condition, was elevated in *Hdc*-KO mice and by amphetamine pretreatment (2-way ANOVA: main effect of genotype: $F[1,4]=8.512$, $p=0.04$; main effect of amphetamine: $F[1,4]=96.28$; $p<0.001$; genotype × amphetamine interaction: $F[1,4]=26.59$; $p=0.007$). (B) Elevated pT202/Y204-ERK1/2 was also seen by Western blotting in *Hdc*-KO mice and after amphetamine (Main effect of genotype: $F[1,14]=10.47$; $p=0.006$; main effect of amphetamine: $F[1,14] =130.7$; $p<0.0001$).

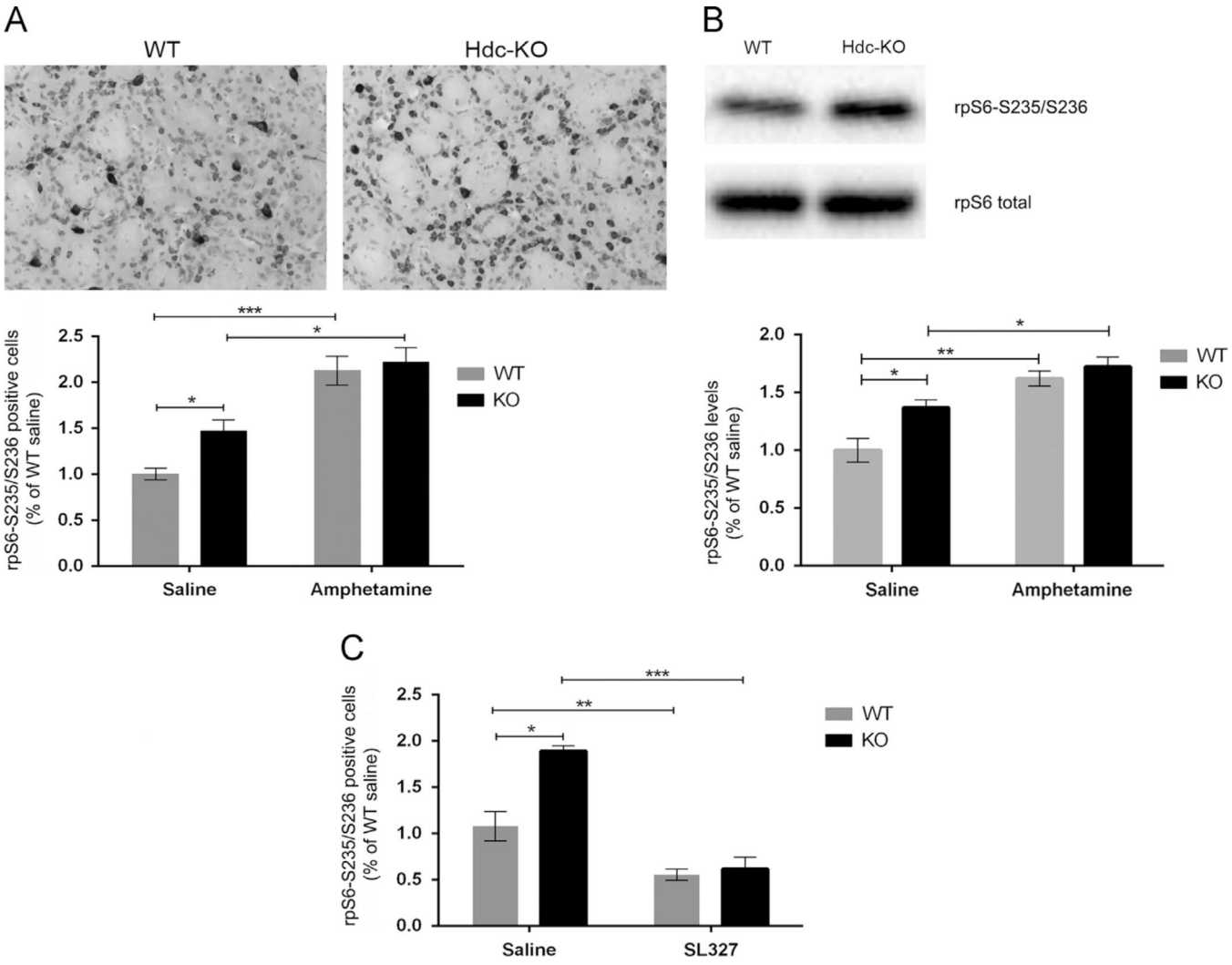

Figure 5.

rpS6 Activation by ERK in *Hdc*-KO mice. (A) Phospho-S235/236 rpS6, which is regulated by MAPK, was elevated in the dorsal striatum in *Hdc*-KO mice and after amphetamine, as measured by immunohistochemistry and cell counting by an observer blind to genotype and condition (2-way ANOVA: main effect of genotype: $F[1,4]=19.93$; $p=0.01$; main effect of amphetamine: $F\ [1,4]=39.20$; $p=0.004$). (B) Elevated pS235/236-rpS6 was attenuated by systemic administration of the MAPK kinase inhibitor SL-327, as assayed by immunohistochemistry and cell counting (main effect of genotype: $F[1,4]=79.07$, $p=0.001$; main effect of SL-327: $F[1,4]=222.9$, $p=0.0001$; genotype × SL-327 interaction: $F[1,4]=8.557$, $p=0.04$). (C) Elevated pS235/236-rpS6 in *Hdc*-KO mice and after amphetamine was corroborated by Western blotting of striatal extracts (2-way ANOVA: main effect of genotype: $F[1,14]=16.78$; $p=0.0008$; main effect of amphetamine: $F[1,41]=54.42$; $p<0.0001$; genotype × amphetamine interaction: $F[1,14]=12.64$; $p=0.003$).